# Patient- and Ventilator-Specific Modeling to Drive the Use and Development of 3D Printed Devices for Rapid Ventilator Splitting During the COVID-19 Pandemic

Muath Bishawi[1,2*], Michael Kaplan[2*], Simbarashe Chidyagwai[2], Jhaymie Cappiello[3], Anne Cherry[4], David MacLeod[4], Ken Gall[5,6], Nathan Evans[6], Michael Kim[6], Rajib Shaha[6], John Whittle[4], Melanie Hollidge[4], George Truskey[2], and Amanda Randles[2]

[1] Department of Surgery, Duke University Medical Center, Durham, NC, USA
[2] Department of Biomedical Engineering, Pratt School of Engineering, Duke University, Durham, NC, USA
[3] Department of Respiratory Therapy, Duke University Medical Center, Durham, NC, USA
[4] Department of Anesthesiology, Duke University Medical Center, Durham, NC, USA
[5] Department of Mechanical Engineering, Pratt School of Engineering, Duke University, Durham, NC, USA
[6] restor3d Inc, Durham NC

**Abstract.** In the early days of the COVID-19 pandemic, there was a pressing need for an expansion of the ventilator capacity in response to the COVID19 pandemic. Reserved for dire situations, ventilator splitting is complex, and has previously been limited to patients with similar pulmonary compliances and tidal volume requirements. To address this need, we developed a system to enable rapid and efficacious splitting between two or more patients with varying lung compliances and tidal volume requirements. We present here a computational framework to both drive device design and inform patient-specific device tuning. By creating a patient- and ventilator-specific airflow model, we were able to identify pressure-controlled splitting as preferable to volume-controlled as well create a simulation-guided framework to identify the optimal airflow resistor for a given patient pairing. In this work, we present the computational model, validation of the model against benchtop test lungs and standard-of-care ventilators, and the methods that enabled simulation of over 200 million patient scenarios using 800,000 compute hours in a 72 hour period.

**Keywords:** airflow · cloud computing · ventilator modeling.

## 1 Introduction

The COVID19 pandemic has shed light on the need for emergency ventilator systems which can be rapidly deployed when the demand for ventilators surpasses

ICCS Camera Ready Version 2022
To cite this paper please use the final published version:
DOI: 10.1007/978-3-031-08757-8_13

their supply [1], such as during regional emergencies [2], global pandemics [3], and in low-resource ICUs [4]. These various scenarios require a ventilator sharing strategy that maximizes the number of patients able to receive potentially life-saving treatment from a limited number of ventilators. Ventilator splitting has been introduced as a strategy to support multiple patients on the same ventilator and has been implemented at a number of institutions during dire situations [5–7]. Recent advances, such as the addition of resistors [8], clamps [9], and valves [10], has allowed ventilator splitting to be useful for carefully matched patients [7]. However, ventilator splitting cannot be safely and rapidly implemented for patients with significantly differing pulmonary compliances [11] or minute ventilation requirements [10], as this could lead to volutrauma, barotrauma, and/or hypoventilation of one or both of the patients. Concerns related to the safety of ventilator splitting has prevented it from being recommended as a general solution for ventilator shortages in the most extreme of circumstances [12].

To address this problem, we developed a rapidly deployable, simple, and low-cost ventilator splitter and resistor system (VSRS) with 3D-printed interchangeable airflow resistors and a clinical support mobile app informed by over 200 million individual simulations to allow for patients with differing pulmonary mechanics to share the same ventilator. A standard ventilator is able to be retrofitted to a split ventilator configuration with the addition of only two essential 3D-printed components, the splitter, which connects one standard ventilator tubing inlet to two tubing outlets, and the resistor. The resistors allow independent differential control over the tidal volumes and pressures delivered to each patient and a computational model was created to quantify how ventilator settings, endotracheal tube diameters, and patient pulmonary compliances affect delivered tidal volumes and pressures with the VSRS. When used together, the 3D printed components and the numerical modelling allow clinicians to quickly, but safely ventilate multiple patients, even when the patients have differing ventilatory requirements and pulmonary compliances. While we present the novel VSRS here, we specifically focus on the role of the computational model. In this work, we present the development of a computational model to simulate air flow in the VSRS and guide usage decisions, validation of the model against benchtop experiments with test lungs, use of the model to determine that safest splitting is pressure-driven as opposed to volume-driven, and finally use of a massively parallel cloud-based framework to pre-compute a wide expance of clinically relevant scenarios.

## 2 Methods

### 2.1 Design of the ventilator splitter and resistor system

The VSRS we developed consists of two primary components: the splitter and the resistor, shown in Figure 1 (b). The splitter component is a Y-shaped adaptor that splits a single airflow into two separate channels (used for the inspiratory limb splitting). When used in reverse, the splitter can combine airflow from two

ICCS Camera Ready Version 2022
To cite this paper please use the final published version:
DOI: 10.1007/978-3-031-08757-8_13

channels into a single channel (used for the expiratory limb). The splitter has a continuously graded diameter such that the interior diameter of the splitter's single-channel end fits over the exterior diameter of standard ventilator tubing, while the exterior diameters of the splitter's dual-channel ends fit within the interior diameter of standard ventilator tubing. The splitter features a 60° junction between the two dual-channel ends. The splitter fits standard ventilator tubing and at least two splitters would be required within a shared ventilator circuit.

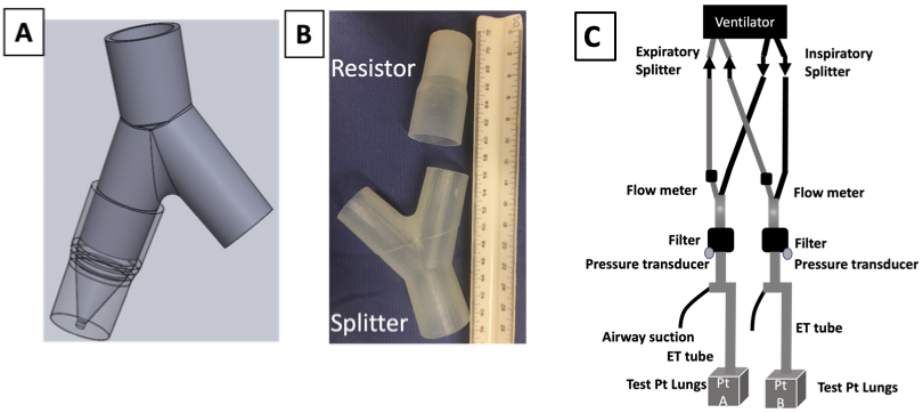


Fig. 1: **Splitter and resistor design and test circuit configuration** :(1A) Overall design, (1B) 3D printed components and (1C) Benchtop circuit setup to capture two patients with different lung compliances

The components of the VSRS are manufactured from a commercially available photopolymer via highly accurate stereolithography (SLA), using a commercially available printer (FormLabs 2, Formlabs Inc, Somerville, MA). This method creates highly reproducible air flow tubes, with a printing dimensional accuracy of approximately 0.5% of the diameter. All prints were done at restor3d (Durham, NC) following their internal quality system for resin-based 3D printing.

### 2.2 Reduced order ventilator computational model

Numerical Model. A pressure-controlled and volume-controlled ventilator were considered for the computational model. A range of Reynolds numbers were simulated as a function of the ventilator settings, with higher Reynolds numbers approaching 4000. Air flow from the ventilator source to the patient was modeled using pipe flow dynamics in a gas network. The gas flow through the pipes is governed by the laws of mass, momentum and energy from which the pressure, velocity, density and temperature of the gas volume were solved. The mass conservation relates the mass flow rates to the pressure and temperature of the gas volume by the following relationship[15]:

ICCS Camera Ready Version 2022
To cite this paper please use the final published version:
DOI: 10.1007/978-3-031-08757-8_13

$$\frac{\partial M}{\partial p} \cdot \frac{dp_I}{dt} + \frac{\partial M}{\partial T} \cdot \frac{dT_I}{dt} = \dot{m}_A + \dot{m}_B \tag{1}$$

were $\frac{\partial M}{\partial p}$ is the partial derivative of the mass of the gas flow with respect to pressure at constant temperature and volume. $\frac{\partial M}{\partial T}$ is the partial derivative of the mass of the gas volume with respect to temperature at constant pressure and volume, $p_I$is the pressure of the gas volume, $T_I$ is the temperature and t is time. M is the mas of gas entering the device. $m_A$ and $m_B$ are the mass flow rates to the patients A and B, respectively.

Energy conservation is given by the following relationship[16]:

$$\frac{\partial U}{\partial p} \cdot \frac{dp_I}{dt} + \frac{\partial U}{\partial T} \cdot \frac{dT_I}{dt} = \Phi_A + \Phi_B + Q_H \tag{2}$$

$\frac{\partial U}{\partial p}$ is the partial derivative of the internal energy of the control volume with respect to pressure at constant temperature and volume. $\frac{\partial U}{\partial T}$ is the partial derivative of the internal energy of the control volume with respect to temperature at constant pressure and volume. $\Phi_A$ and $\Phi_B$ are the energy flow rates to the patients. $Q_H$ represents the energy flow rate from the pipe wall. Pressure loses due to viscous friction are given by the momentum balance relationship[17]:

$$\begin{aligned} p_A - p_I &= \left(\frac{\dot{m}_A}{S}\right)^2 \cdot \left(\frac{1}{\rho_I} - \frac{1}{\rho_A}\right) + \Delta p_{AI} \\ p_B - p_I &= \left(\frac{\dot{m}_B}{S}\right)^2 \cdot \left(\frac{1}{\rho_I} - \frac{1}{\rho_B}\right) + \Delta p_{BI} \end{aligned} \tag{3}$$

$p_A$ and $p_B$ are the pressures at the inlet and the outlet of the pipe respectively. $\rho_A$ and $\rho_B$ represent densities at the inlet and outlet of the pipe. S is the cross sectional area and $\Delta p_{AI}$ and $\Delta p_{BI}$ are the pressure loses due to friction.

The two patients are connected to each other by way of a junction, with a resistor connected distal to one of the branches to enable controlling the differential flow. The lungs are modeled as a Hookean spring (modelling the inverse of the compliance of the lungs) and a viscous dashpot (modelling the resistance of the upper respiratory tract) in parallel. This lung model presented in this study is consistent with other studies that have used a resistor - capacitor model to represent the lungs [13]. The simulations were performed using MathWork's Simscape (Simulink v4.8) Foundational Blocks. The ventilator is simulated by a pulse wave form generator with a period corresponding to the respiratory rate and inspiratory time, with a maximum value corresponding to the PIP and minimum value corresponding to the PEEP. In order for the system to reach steady state, at least 5 breath cycles were simulated for each set of parameters. The input parameters used for the numerical model are shown in table 1 and 2.

Parallelization. It was important to not only develop a method that could accurately calculate resulting tidal volume for any two given patients and set

ICCS Camera Ready Version 2022
To cite this paper please use the final published version:
DOI: 10.1007/978-3-031-08757-8_13

ventilator to inform the decision of resistor to choose, but, moreover, overall time-to-solution was critical. It was important to pre-calculate all data so that it could be provided to doctors **in an offline capacity** and easily accessible manner without having to wait on a simulation. The goal was to provide clinicians with the ability to enter minimal information about the patients and the ventilator and receive immediate feedback regarding how to setup the VSRS. To that end, all of the combinations needed to be simulated a priori. To accomplish this, we parallelized the model and deployed it in a Microsoft Azure instance. The use of a cloud-based architecture was a strong fit for our needs based on the ability to configure the infrastructural aggregate to suit the problem at hand. We used 24,000 cores of the Azure individual node type HB60 in a datacenter in Western Europe. While the individual pairings were fundamentally framed as an embarrassingly parallel problem, a tighter coupling was imposed to reduce overall time-to-solution. As the code was built with MATLAB which relies on runtime compilation, the time to compile the code was actually significant compared to the simulation. In order to run the required 270 million simulations to span our search space (Table 2), it was important to reduce the time spent in compilation. We set up a systematic job hierarchy to maximize use of a built-in functionality for sweeping across parameters. We were thus able to pair down 270 million simulations to 146 thousand jobs, with only one compilation per job. All post-processing was completed on-node after the simulation completed to minimize data communication and storage. Only steady-state tidal volume, maximum delivered pressure, and minimum delivered pressure were stored. Lessons learned regarding fast deployment of such models are described in [14].

Table 1: Range of parameters simulated with the computational model

| | **Minimum Value** | **Maximum Value** | **Step Size** |
|---|---|---|---|
| Pulmonary Compliance ($ml/cmH_2O$) | 10 | 100 | 1 |
| Endotracheal Tube Diameter (mm) | 6 | 8.5 | 0.5 |
| Peak Inspiratory Pressure ($cmH_2O$) | 20 | 50 | 1 |
| Positive End - Expiratory Pressure ($cmH_2O$) | 5 | 20 | 1 |
| Inspiratory to Expiratory Ratio | 1:3 | 1:1 | fractional |
| Respiratory Rate (breaths/minute) | 10 | 30 | 1 |
| Resistor Radii (mm) | 2.5 | 5.5 | 0.5 |

### 2.3 Benchtop testing of VSRS using test lungs

Benchtop testing was used to confirm that the VSRS could be used to ventilate two test lungs (Linear Test Lung, Ingmar Medical, Pittsburgh, PA) properly. The measurements from this circuit were used to validate the computational model. The benchtop circuit was used to assess applicability to both standard ICU ventilators and anesthesia machines, both of which could be required during times of ventilator shortages. As shown in Figure 1(c), the circuit incorporated a number of one-way valves at the inspiratory and expiratory limbs to limit mixing and viral/bacterial filters were placed at locations of possible cross contamination.

ICCS Camera Ready Version 2022
To cite this paper please use the final published version:
DOI: 10.1007/978-3-031-08757-8_13

The circuit consisted of two test lungs in which two different compliances were tested during our experiments, as presented in Table 1. Using ventilator settings with a respiratory rate of 20 bpm (breaths per minute), a PEEP (positive end-expiratory pressure) of 5 cmH2O, and PIP (peak inspiratory pressure) of 20 cmH2O, the delivered tidal volumes to the low compliance artificial lung was 352-359 ml and 566-567 ml to the medium compliance lung (Table 2). The precise compliance of the test lungs in 'low' configuration was determined to be 18 ml/cmH2O, and 34-36 ml/cmH2O for the 'medium' configuration (Table 2). Ventilator parameters recorded were: peak inspiratory pressure (cmH2O), mean pressure (cmH2O), tidal volume (mL), and dynamic compliance (mL/cmH2O). Individual test lung circuit parameters recorded (each circuit, A and B) were: distal circuit maximum and trough pressure (mmHg), using a dry disposable pressure transducer (Transpac IV, ICU Medical, San Clemente, CA) connected directly to the gas sample port of each distal circuit filter. Pressures were recorded using a GE Carescape Monitor. Each distal circuit tidal volume was measured using in-line volume monitors (Ohmeda 6800 Volume Monitor, Bird Products, Palm Springs, CA). A similar method of validating the benchtop setup for use on two test lungs with different compliances was demonstrated by, [10].

Table 2: Individual test lung mechanics using the single circuit set up

| | **Patient A Low Compliance** | **Patient B Low Compliance** | **Patient A Medium Compliance** | **Patient B Medium Compliance** |
|---|---|---|---|---|
| Compliance | 18 | 18 | 34 | 36 |
| Pressure (Peak/Low) | 26/13 | 26/13 | 25/13 | 25/13 |
| Tidal Volume | 352 | 359 | 566 | 567 |

## 3 Results

### 3.1 The computational model predicts benchtop measurements

The computational model was validated against the test lung data for multiple different pulmonary compliance values, respiratory rates, and resistor sizes. There is excellent agreement between the computational model and the test lung data, which is evidenced by a Pearson correlation coefficient of 0.9697 and a p-value of less than 0.0001. Figure 2 illustrates the comparison between simulated and benchtop data for one set of lung compliances and respiratory rates, while varying the resistor sizes. Both the benchtop data and the computational model agree that a 3.5 mm resistor on the higher compliance limb will result in equivalent delivered tidal volumes to both lungs for this specific configuration.

More generally, the computational model supports the findings from the benchtop model that adding a resistor to the split ventilator circuit significantly

ICCS Camera Ready Version 2022
To cite this paper please use the final published version:
DOI: 10.1007/978-3-031-08757-8_13

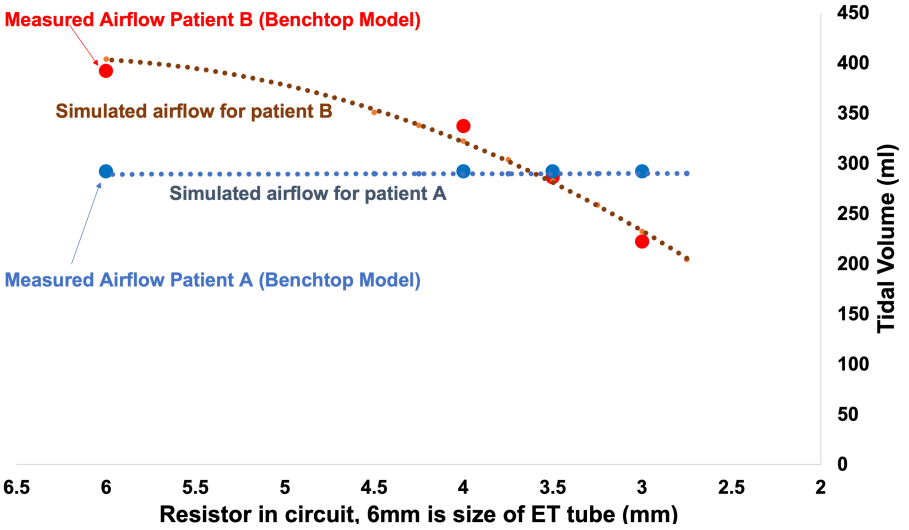


Fig. 2: **Comparison of the numerical results to the benchtop experimental data** Comparison of the simulation results (dotted lines) with the benchtop results (large circles) for patient A (medium compliance) and patient B (low compliance). Both are in agreement over a range of resistor sizes and demonstrate similar delivered tidal volumes to both patients using a 3.5 mm resistor.

alters delivered tidal volumes and pressures. Figure 3 illustrates the model outputs of predicted pressure, flow rate, and volume waveforms for a patient with a lower pulmonary compliance (Patient A) sharing a ventilator with a patient with higher pulmonary compliance and a resistor (Patient B). The characteristic waveform of pressure-controlled ventilation is observed for patient A, where the ventilator reaches the ventilator-specified peak inspiratory pressure and then a plateau occurs. However, for patient B, the resistor slows the buildup of pressure and the ventilator-specified peak inspiratory pressure is never reached. As a result, the flow rate waveform for patients A and B markedly differ, and as demonstrated, the computational model is able to accurately capture the effect of different resistor sizes on the resulting tidal volume for each patient.

### 3.2 Pressure-controlled ventilation protects patients from changes in the opposing patients circuit

The computational model was also used to improve the design of the VSRS. In particular, there was an outstanding question regarding whether the ventilator splitting should be pressure-controlled or volume-controlled. The validated computational model allowed this question to be resolved through comparison of simulations in each case. Figure 4 (a) illustrates how in pressure-controlled ventilation both the tidal volumes and pressures to patient A are not affected by changes to patient B's circuit, such as the addition of a resistor, which was a trend also

ICCS Camera Ready Version 2022
To cite this paper please use the final published version:
DOI: 10.1007/978-3-031-08757-8_13

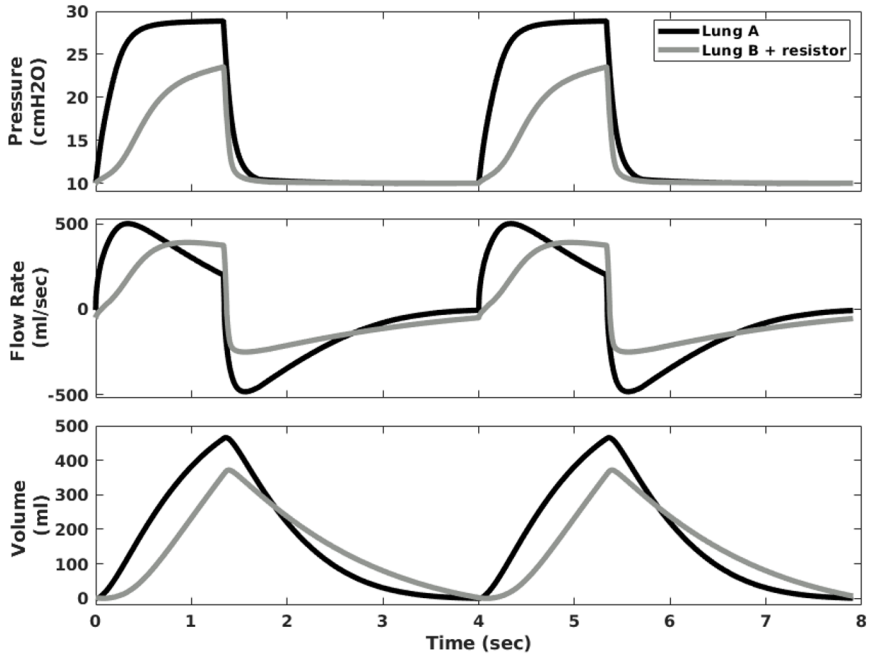


Fig. 3: **Model output waveforms for pressure, flow rate, and tidal volume** Example model output for simulated patient A (compliance of 30 ml/cmH2O) and simulated patient B (compliance of 75 ml/cmH2O) using a 4 mm resistor. While Patient A experiences the peak inspiratory pressure set by the ventilator, the presence of the resistor results in decreased peak pressures to Patient B.

observed in the benchtop data. In both pressure-controlled and volume-controlled ventilation, the pressure delivered to the bifurcation at the circuit is always equal to each branch, and therefore the delivered tidal volumes to each patient are independently a function of how their pulmonary characteristics respond to this pressure. However, in volume-controlled ventilation, we demonstrate that a coupling of the delivered tidal volumes between the two patients occurs. When the resistance of one limb of the circuit increases, such as through a kink in tubing or secretions, the ventilator senses the resulting decrease in combined delivered tidal volume and subsequently increases the delivered pressures in an attempt to achieve the desired tidal volume, which results in increased pressures and volumes to both patients. This differs from pressure-controlled ventilation, where patient A is protected from experiencing dangerously elevated pressures and tidal volumes in response to changes in resistance in patient B's circuit (Figure 4 (a)). Therefore, we show that pressure-controlled ventilator splitting offers a markedly improved safety profile due to a reduced risk of barotrauma or volutrauma to one patient from changes in the opposite patient's circuit.

ICCS Camera Ready Version 2022
To cite this paper please use the final published version:
DOI: 10.1007/978-3-031-08757-8_13

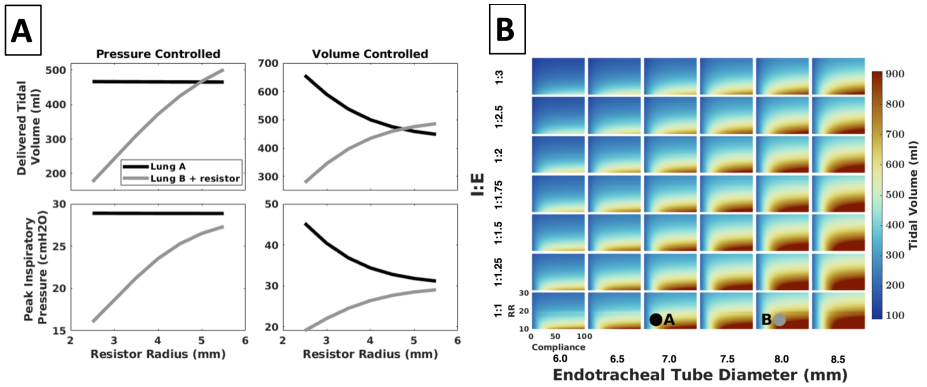


Fig. 4: **(A) Comparing pressure-controlled and volume-controlled ventilation in the split ventilator configuration** Computational model output of tidal volume (top row) and peak inspiratory pressure (bottom row) for different resistor sizes under pressure-controlled ventilation (left column) and volume-controlled ventilation (right column). **(B) Multiple dimensions of nonlinearity for predicted tidal volumes** The predicted volumes for a 8.5 mm endotracheal tube compared to a 6 mm endotracheal tube as a function of pulmonary compliance and respiratory rate with other ventilator settings held constant (PIP of 28, PEEP of 8, I:E of 1).

While this finding was significant in driving VSRS usage setup in a manner to better protect the patient, it also had implications for our computational model. Because the patients could be viewed as decoupled under a pressure-controlled setup, we could assume no interaction between patients on the same ventilator and subsequently decouple the simulations as well. Functionally, this finding led to a drastic reduction in the number of parameter pairings that needed to be simulated and allowed us to restrict our search space.

### 3.3 Tidal volumes from pressure-controlled ventilation are highly sensitive to small changes in ventilator settings, endotracheal tube sizes, and patient characteristics

Predicted tidal volumes from pressure-controlled ventilation are sensitive to small changes in multiple parameters (Table 1) in a non-linear fashion (Figure 4 (b)). At lower compliance values, different endotracheal tube sizes result in only minimal changes in tidal volumes and tidal volumes increase roughly linearly with compliance.

However, as Figure 4 (b) illustrates, for larger compliance values there is a marked change in the increase in tidal volume as a function of pulmonary compliance and significant differences in tidal volumes due to different endotracheal tube sizes can occur. This is an important characteristic to consider as pulmonary compliance is expected to change due to disease progression or

ICCS Camera Ready Version 2022
To cite this paper please use the final published version:
DOI: 10.1007/978-3-031-08757-8_13

recovery. For example, safe tidal volumes for a given set of patient characteristics and ventilator settings while the patient has low pulmonary compliance would become dangerously high as the patient improves, and therefore a different resistor size needs to be used. Figure 4 (b) also demonstrates the non-linear effect of respiratory rate (RR) on tidal volumes, where the sensitivity of tidal volumes to changes in RR is much greater for lower RRs than for higher RRs. These and other non-linearities necessitate a high-resolution parameter exploration in order to safely and precisely quantify the effect of multiple patient parameters and ventilator settings on delivered tidal volumes. These experiments emphasize how small changes in patient-specific parameters can lead to large changes in delivered tidal volumes. Given the large parameter space required to explore how these patient-specific parameters affect tidal volumes, a computational model was needed to make the exploration of such a large parameter space feasible in a short period of time.

### 3.4 The computational model solves the large parameter space of potential patient pairings

To properly account for the range of different factors influencing patient-delivered tidal volumes in a split-ventilator configuration, we performed the largest-to-date computational effort to simulate the necessary number of different ventilator settings and patient-specific parameters that clinicians may encounter. Figure 5 displays the results of exploring the seven-dimensional parameter space (Table 1) which were found to significantly affect predicted tidal volumes and pressures. 270 million different simulations were required to explore the parameter space at a sufficient resolution such that the step size for a given parameter resulted in less than a 5% change in tidal volume.

Figure 5 depicts the scale of the parameter sweep that was performed. The left panel of Figure 5 shows how increasing the driving pressure (PIP-PEEP), as well as increasing the I:E and therefore the inspiratory time, acts to increase tidal volumes. The right panel of Figure 5 is an expansion of the predicted tidal volumes of the upper left panel by selecting a PIP of 28, PEEP of 8, and I:E of 1 and illustrating tidal volumes as a function of endotracheal tube sizes, RR, and compliance. The interplay of multiple parameters is observed as the effect of changing RR on tidal volumes is itself dependent on the patient's pulmonary compliance and endotracheal tube size. To complete these simulations, 24,000 cores were used over a 72 hour period using more then one million core hours in Microsoft Azure.

## 4 Discussion and Conclusion

Shared ventilatory support still poses significant risk of harm and should not be undertaken unless there are no other viable options. However, the dire circumstances during the COVID-19 pandemic has brought renewed interest [15] and innovation [10], [11] in ventilator sharing, which has applications in future

ICCS Camera Ready Version 2022
To cite this paper please use the final published version:
DOI: 10.1007/978-3-031-08757-8_13

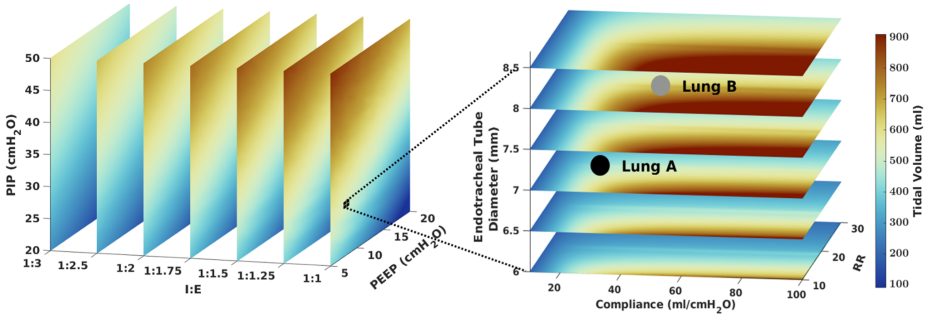


Fig. 5: **Illustration of the results from computational model's parameter sweep** Left: The average tidal volume without a resistor for all simulations as a function of PIP, PEEP, and I:E. Right: Average tidal volume without a resistor for all simulations originating from the black square on the upper left figure (PIP of 28, PEEP of 8, I:E of 1) as a function of RR, compliances, and endotracheal tube diameters.

respiratory outbreaks, the battlefield, and in low resource ICU settings, as well as during the current global pandemic. The proposed VSRS relies exclusively on simple 3D printed components that can be readily created in locations with a 3D printer and shipped to nearby hospitals, as well as a free mobile app that removes the guess work from deciding how to pair patients and what resistor size to use. In this work, we demonstrate the role that a computational fluid dynamics model can play in guiding system design and VSRS use.

The computational model was able to demonstrate the large difference in delivered airflow to two lungs of different compliances sharing the same ventilator without use of the VSRS. This confirms the feared clinical scenario that would lead to one patient potentially experiencing volutrauma and/or the other having inadequate ventilation. Using 3D printed airflow resistors in the circuit for the patient with the higher compliance lungs allows for control over the delivered tidal volume to the higher compliance lung. We showed that a pressure-controlled splitting using the VSRS can reduce the effects of one patient's ventilation on the other in a shared ventilator setting. Moreover, we confirmed that the airflow can be predicted using the computational model we have developed, which allows clinicians to select the resistor that will result in the desired tidal volumes for each patient, even for patients with very different ventilation needs and pulmonary compliances. By leveraging large-scale cloud resources, we were able to pre-compute results for 270 million potential clinical scenarios to be fed into a mobile app that has already been created to assist clinicians with this process, [14].

This study has a number of important limitations. Mainly, we have not tested this system on real patients during ventilator splitting. A patient's pulmonary mechanics might have subtle differences compared to the simplifications implicit in the test lung and computational model. For example, the model does not simulate

ICCS Camera Ready Version 2022
To cite this paper please use the final published version:
DOI: 10.1007/978-3-031-08757-8_13

the effect of alveolar recruitment, and therefore increasing PEEP at a given PIP never results in increased tidal volumes. Additionally, the current version of the VSRS excludes of the effects of differing patient pulmonary resistances, which we found to be secondary compared to the effect of pulmonary compliances, but can be included in a new version of the computational model at a future date.

The VSRS is designed to initially have the patient on a single ventilator in order to determine their patient-specific pulmonary compliance and, in the case of volume-controlled ventilation, resistance. Once the patient is stabilized, they then can be moved to a split ventilator configuration using the VSRS for longer term ventilatory support with their now known patient-specific pulmonary characteristics entered into the app in order to choose the proper resistor size. It will be important to redetermine the optimal resistor and ventilator settings as the patients' conditions can change rapidly with time, which can be accomplished done by temporarily occluding air flow to one of the patients for a few breaths to determine the pulmonary compliance for the other patient. The developed computational model can then be used to rapidly recalculate optimal resistor and ventilator settings.

However, the goal behind ventilator splitting is to address periods of short supply, especially given reports of prolonged ventilator support times for COVID-19 patients. Reserved for dire situations, ventilator splitting is complex, and introduces many safety concerns related to the lack of control over individual patient's respiratory support, some of which are alleviated by the VSRS. By precomputing the hundreds of millions of different possible combinations of ventilator settings and patient-specific characteristics and by taking advantage of simple 3D printable geometries, the VSRS can be rapidly deployed at minimal cost wherever the need for ventilators surpasses their supply.

## 5 Acknowledgements:

The authors would like to thank the COVID-19 HPC Consortium for both the compute hours and the broader Microsoft team for all of the support. They would like to thank T. Milledge, C. Kneifel, V. Orlikowski, J. Dorff, and M. Newton for critical computing support.

## References

1. Optimizing ventilator use during the covid-19 pandemic. `https://www.hhs.gov/sites/default/files/optimizing-ventilator-use-during-covid19-pandemic.pdf`, accessed: 2020-04-20
2. Wilgis, J.: Strategies for providing mechanical ventilation in a mass casualty incident: distribution versus stockpiling. Respiratory care **53**(1), 96–103 (2008)
3. Truog, R.D., Mitchell, C., Daley, G.Q.: The toughest triage—allocating ventilators in a pandemic. New England Journal of Medicine **382**(21), 1973–1975 (2020)
4. Guérin, C., Lévy, P.: Easier access to mechanical ventilation worldwide: an urgent need for low income countries, especially in face of the growing covid-19 crisis (2020)

ICCS Camera Ready Version 2022
To cite this paper please use the final published version:
DOI: 10.1007/978-3-031-08757-8_13

5. Hadar, S.S., Yarden, S., Leav, O.A., Gilad, M., Joseph, K., Leshem, N., Neta, Z., Naor, M., Amir, B., Rotem, L.: Adaptive split ventilator system enables parallel ventilation, individual monitoring and ventilation pressures control for each lung simulators. medRxiv (2020)
6. Tronstad, C., Martinsen, T., Olsen, M., Rosseland, L., Pettersen, F., Martinsen, Ø., Høgetveit, J., Kalvøy, H.: Splitting one ventilator for multiple patients–a technical assessment (2020)
7. Beitler, J.R., Mittel, A.M., Kallet, R., Kacmarek, R., Hess, D., Branson, R., Olson, M., Garcia, I., Powell, B., Wang, D.S., et al.: Ventilator sharing during an acute shortage caused by the covid-19 pandemic. American journal of respiratory and critical care medicine **202**(4), 600–604 (2020)
8. Lai, B.K., Erian, J.L., Pew, S.H., Eckmann, M.S.: Emergency open-source three-dimensional printable ventilator circuit splitter and flow regulator during the covid-19 pandemic. Anesthesiology **133**(1), 246–248 (2020)
9. Clarke, A., Stephens, A., Liao, S., Byrne, T., Gregory, S.: Coping with covid-19: ventilator splitting with differential driving pressures using standard hospital equipment. Anaesthesia **75**(7), 872–880 (2020)
10. Srinivasan, S.S., Ramadi, K.B., Vicario, F., Gwynne, D., Hayward, A., Lagier, D., Langer, R., Frassica, J.J., Baron, R.M., Traverso, G.: A rapidly deployable individualized system for augmenting ventilator capacity. Science Translational Medicine **12**(549), eabb9401 (2020)
11. Clarke, A.: 3d printed circuit splitter and flow restriction devices for multiple patient lung ventilation using one anaesthesia workstation or ventilator. Anaesthesia **75**(6), 819–820 (2020)
12. Joint statement on multiple patients per ventilator. `https://www.asahq.org/about-asa/newsroom/news-releases/2020/03/joint-statement-on-multiple-patients-per-ventilator.`, accessed: 2020-04-25
13. Schmidt, M., Foitzik, B., Hochmuth, O., Schmalisch, G.: Computer simulation of the measured respiratory impedance in newborn infants and the effect of the measurement equipment. Medical engineering & physics **20**(3), 220–228 (1998)
14. Kaplan, M., Kneifel, C., Orlikowski, V., Dorff, J., Newton, M., Howard, A., Shinn, D., Bishawi, M., Chidyagwai, S., Balogh, P., et al.: Cloud computing for covid-19: lessons learned from massively parallel models of ventilator splitting. Computing in Science & Engineering **22**(6), 37–47 (2020)
15. Cherry, A.D., Cappiello, J., Bishawi, M., Hollidge, M.G., MacLeod, D.B.: Shared ventilation: toward safer ventilator splitting in resource emergencies. Anesthesiology **133**(3), 681–683 (2020)

ICCS Camera Ready Version 2022
To cite this paper please use the final published version:
DOI: 10.1007/978-3-031-08757-8_13